Optical MIMO transmission for SCFDM-PON based on polarization interleaving

Bangjiang Lin (林邦姜), Juhao Li (李巨浩)*, Hui Yang (杨 慧), Lixin Zhu (朱立新), Yongqi He (何永琪), and Zhangyuan Chen (陈章渊)**

State Key Laboratory of Advanced Optical Communication Systems and Networks, Peking University, Beijing 100871, China

**Corresponding author: juhao_li@pku.edu.cn; **corresponding author: chenzhy@pku.edu.cn*

Received April 21, 2012; accepted July 10, 2012; posted online October 24, 2012

Orthogonal frequency division multiplexing-passive optical network (OFDM-PON) and single-carrier frequency division multiplexing (SCFDM)-PON are promising solutions for future high-speed PON-based access. A polarization division multiplexing scheme with direct detection is proposed for OFDM-PON to effectively reduce bandwidth requirements for components. However, the scheme strictly requires spectrum overlapping of two orthogonal sidebands and the 4×4 multi-input-multi-output (MIMO) algorithm to eliminate complex cross-polarization interference. In this letter, we propose a polarization interleaving (PI) approach that significantly reduces bandwidth requirements for optical and electrical components while achieving a high-flexibility and low-complexity MIMO algorithm. Downstream single sideband PI-SCFDM transmission is experimentally demonstrated.

OCIS codes: 060.2330, 060.4250.
doi: 10.3788/COL201210.120602.

In the future, next-generation optical access networks will migrate to a capacity of 40 Gb/s or even higher per channel. Passive optical networks (PONs) based on orthogonal frequency division multiplexing (OFDM) and single-carrier frequency division multiplexing (SCFDM) have recently received considerable attention because these networks present strong resistance to fiber dispersion, high spectral efficiency, and extreme flexibility in terms of multiple service access and dynamic bandwidth allocation[1−9]. SCFDM is a modified form of OFDM. Given its inherent single-carrier transmission characteristics, it has a lower peak-to-average ratio than does OFDM. Experiments have shown that SCFDM exhibits better performance[10].

The polarization division multiplexing (PDM) OFDM-PON scheme with direct detection has recently been proposed to reduce bandwidth requirements for components[11−13]. However, the scheme strictly requires spectrum overlapping of two orthogonal sidebands and the 4×4 multi-input-multi-output (MIMO) channel estimation algorithm to eliminate complex cross-polarization interference. In this letter, we propose a polarization interleaving (PI) approach for SCFDM-PON based on direct detection. This approach significantly reduces bandwidth requirements for optical and electrical components while achieving a similar 2×2 MIMO algorithm with PDM coherent optical (CO) OFDM[14]. Downstream PI-SCFDM-PON is experimentally demonstrated to show the feasibility of the proposed scheme. Compared with PDM, the PI scheme realizes a high-flexibility and low-complexity MIMO algorithm at the cost of slightly reduced spectral efficiency. The MIMO algorithm can be easily extended to OFDM-PON.

Figure 1 shows the schematic of the proposed PI approach. At the transmitter, an intensity modulator (IM) is driven by a radio frequency (RF) $f_0/2$ with carrier suppression to generate two optical carriers with frequency spacing f_0. Then, an interleaver is used to separate the two carriers. For each SCFDM transmitter, the baseband SCFDM signals are up-converted by digital or analog IQ modulation. The up-converted signals can be expressed as

$$d_x = \sum_{i=1}^{N} S_{1,i}(t) \exp(\mathrm{j}2\pi f_\mathrm{u} t), \tag{1}$$

$$d_y = \sum_{i=1}^{N} S_{2,i}(t) \exp(\mathrm{j}2\pi f_\mathrm{u} t), \tag{2}$$

where $S_{1,i}$ and $S_{2,i}$ denote the baseband SCFDM signals of the ith subcarrier modulated in SCFDM transmitters 1 and 2, respectively; f_u is the RF carrier; N is the number of subcarriers. The electrical SCFDM signals are converted to optical double sideband (DSB) signals by optical IMs. Figures 1(a) and (b) show the schematic outputs of the two IMs. Then, the signals are combined

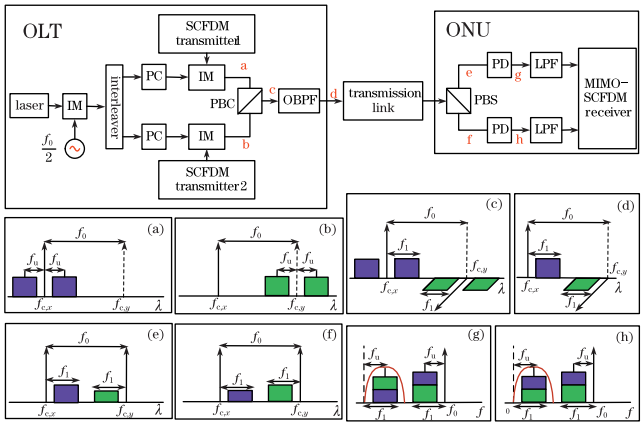

Fig. 1. Architecture of PI-SCFDM-PON. PC: polarization controller.

by the polarization beam combiner (PBC) and converted to single sideband (SSB) signals by an optical bandpass filter (OBPF). The SSB optical signals obtained after filtering can be written as

$$S_x = A_x \sum_{i=1}^{N} S_{1,i}(t) \exp[\mathrm{j}2\pi(f_{\mathrm{c},x}+f_{\mathrm{u}})t] + B_x \exp(\mathrm{j}2\pi f_{\mathrm{c},x}t), \tag{3}$$

$$S_y = A_y \sum_{i=1}^{N} S_{2,i}(t) \exp[\mathrm{j}2\pi(f_{c,y}-f_{\mathrm{u}})t] + B_y \exp(\mathrm{j}2\pi f_{\mathrm{c},y}t), \tag{4}$$

where $f_{\mathrm{c},x}$ and $f_{\mathrm{c},y}$ denote the two PI optical carriers; A_x, B_x, and A_y, B_y represent the amplitudes of the SCFDM signals and optical carriers. Frequency spacing f_0 should be larger than $2f_1$ (Fig. 1(d)). At the receiver, the optical PI-SCFDM signals are split by the polarization beam splitter (PBS), and each output consists of an arbitrary mix of two transmitted SCFDM signals (Figs. 1(e) and (f)). After direct detection by two photodiodes (PDs), various frequency components interfere with one another and the two outputs can be expressed as

$$\begin{aligned} S'_x = &\sum_{i=1}^{N} a_{11}(i) S_{1,i}(t) \exp(\mathrm{j}2\pi f_{\mathrm{u}}t) \\ &+ \sum_{i=1}^{N} a_{12}(i) S_{2,i}(t) \exp(\mathrm{j}2\pi f_{\mathrm{u}}t) + I_x \exp(\mathrm{j}2\pi f_0 t) \\ &+ \sum_{i=1}^{N} b_{x,1}(i) S_{1,i}(t) \exp[\mathrm{j}2\pi(f_0 - f_{\mathrm{u}})t] \\ &+ \sum_{i=1}^{N} b_{x},2(i) S_{2,i}(t) \exp[\mathrm{j}2\pi(f_0 - f_{\mathrm{u}})t], \end{aligned} \tag{5}$$

$$\begin{aligned} S'_y = &\sum_{i=1}^{N} a_{21}(i) S_{1,i}(t) \exp(\mathrm{j}2\pi f_{\mathrm{u}}t) \\ &+ \sum_{i=1}^{N} a_{22}(i) S_{2,i}(t) \exp(j2\pi f_{\mathrm{u}}t) + I_y \exp[\mathrm{j}2\pi f_0 t] \\ &+ \sum_{i=1}^{N} b_{y,1}(i) S_{2,i}(t) \exp[\mathrm{j}2\pi(f_0 - f_{\mathrm{u}})t] \\ &+ \sum_{i=1}^{N} b_{y,2}(i) S_{1,i}(t) \exp[\mathrm{j}2\pi(f_0 - f_{\mathrm{u}})t], \end{aligned} \tag{6}$$

where I_x and I_y denote the beating interferences of two optical carriers for each polarization. The beating between the two optical carriers and two signal sidebands for each polarization results in four groups of electrical signals. a_{11}, a_{12}, $b_{x,1}$, $b_{x,2}$ denote the channel response coefficients of each group of signals in POL-X; a_{21}, a_{22}, $b_{y,1}$, $b_{y,2}$ are analogous for POL-Y. Because frequency spacing f_0 is larger than $2f_1$, the high-frequency signals that satisfy $f > f_1$ can be filtered by two low-pass filters (LPFs), as shown in Figs. 1(g) and (h). Thus, the final received electrical signals can be expressed as

$$\begin{aligned} d'_x = &\sum_{i=1}^{N} a_{11}(i) S_{1,i}(t) \exp(\mathrm{j}2\pi f_{\mathrm{u}}t) \\ &+ \sum_{i=1}^{N} a_{12}(i) S_{2,i}(t) \exp(\mathrm{j}2\pi f_{\mathrm{u}}t), \end{aligned} \tag{7}$$

$$\begin{aligned} d'_y = &\sum_{i=1}^{N} a_{21}(i) S_{1,i}(t) \exp(\mathrm{j}2\pi f_{\mathrm{u}}t) \\ &+ \sum_{i=1}^{N} a_{22}(i) S_{2,i}(t) \exp(\mathrm{j}2\pi f_{\mathrm{u}}t). \end{aligned} \tag{8}$$

The system can be regarded as a MIMO system with two inputs and two outputs. For each subcarrier, the received signal before MIMO processing can be expressed as

$$\begin{pmatrix} d'_x(i) \\ d'_y(i) \end{pmatrix} = \begin{pmatrix} a_{11}(i) & a_{12}(i) \\ a_{21}(i) & a_{22}(i) \end{pmatrix} \begin{pmatrix} d_x(i) \\ d_y(i) \end{pmatrix} + \begin{pmatrix} n_x(i) \\ n_y(i) \end{pmatrix}, \tag{9}$$

where $n_x(i)$ and $n_y(i)$ are the frequency-domain noise within the subcarrier in the two received signals. The MIMO algorithm for recovering original data is similar to that used in CO PDM OFDM systems[14−16]. The frequency spacing between polarizations can be reduced if high-order QAM mapping is applied.

Figure 2 shows the experimental setup for downstream SSB PI-SCFDM transmission. At the transmitter, two 3-Gbaud baseband quadrature phase-shift keying (QPSK) SCFDM signals are up-sampled four times and then up-converted to 3 GHz by digital I-Q modulation. In its modified form, the baseband digital signal processing (DSP) method of SCFDM is similar to that of OFDM, as discussed in Ref. [1]. The total number of subcarriers is 256, of which 210 are used for data transmission. The cyclic prefix (CP) has a length of 16. Before the signals

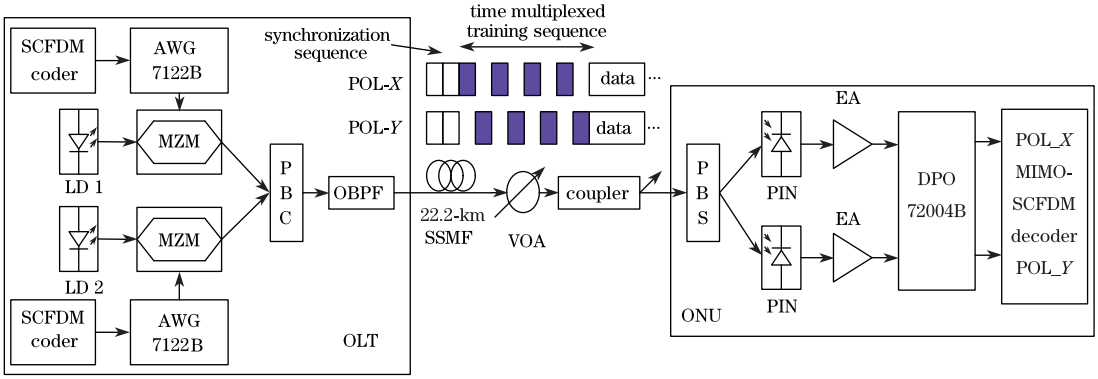

Fig. 2. Experimental setup for downstream SSB PI-SCFDM transmission. LD: laser diode.

are transmitted, preambles are added for synchronization and MIMO channel estimation. For each polarization, the preambles include two synchronization sequences and four time-multiplexed training sequences. The total length of the synchronization sequence is 42.7 ns, which includes two Chu sequences. Each time-multiplexed training sequence consists of 256 specific symbols, a 16-symbol CP, and a 272-symbol zero sequence. The total length of the training sequence is 725.3 ns. The preamble is incorporated after every 200 SCFDM symbols. The generated waveforms are uploaded into the arbitrary waveform generator (Tektronix AWG7122B) operating at 12 GS/s. To generate the two optical carriers, we can adopt a method similar to interleaving and intensity modulation driven by a RF signal[12]. In our experiment, we use two tunable lasers to facilitate generation. Our scheme differs from the conventional WDM scheme in that the two optical carriers are in the same channel, thereby presenting considerably less frequency spacing than that generated with two WDM channels. Moreover, the multiplexing and demultiplexing of the two optical carriers are realized using the PBC and PBS, which can be easily integrated into an optical transceiver. By contrast, a tunable filter is required to separate two WDM channels. The linewidths of the two lasers are 5 kHz, and the wavelengths are set to 1549.753 and 1550.042 nm, respectively. Two intensity Mach–Zehnder modulators (MZMs) are used to convert the two SCFDM signals to DSB optical signals. Then, the signals are combined by a PBC. An OBPF is used to convert the DSB signal to a SSB signal. The optical distribution network is simulated using a 22.2-km standard single-mode fiber (SSMF), a variable optical attenuator (VOA), and a 50/50 coupler. At the receiver, the SSB PI-SCFDM signals are split by a PBS and then detected by two PDs. The electrical RF SCFDM signals are amplified by two electrical amplifiers (EAs) prior to sampling by using the real-time digital storage oscilloscope (Tektronix DPO72004B) operating at 50 GS/s. Given that the bandwidths of the two EAs are less than 5 GHz, they also serve as LPFs. The sampled SCFDM signals are digitally down-converted. After synchronization, the CP is removed and the SCFDM signals are transformed into frequency-domain signals by 256-point DFT. The cross-polarization interferences are removed by MIMO channel equalization. The equalized SCFDM signals are transformed into time-domain signals by 210-point IDFT for further study.

The optical spectra under back-to-back (B2B) transmission are shown in Fig. 3. Figures 3(a) and (b) illustrate the outputs of the two MZMs. The difference in the two optical spectra is induced because the two driver amplifiers that we use in our experiment have different gain shapes. The optical spectrum after multiplexing with the PBC is shown in Fig. 3(c). Figure 3(d) shows the optical spectrum after the OBPF. Figures 3(e) and (f) show the optical spectra of Pol-X' and Pol-Y', respectively. Each output of the PBS is the mix of both polarization components. Figures 3(g) and (h) depict the electrical spectra of the SCFDM signals. Figure 4 shows the bit error rate (BER) performance versus the received optical power before multiplexing by the PBS. The inset shows the constellations for both polarizations with −8.5-dBm received power after 22.2-km fiber transmission.

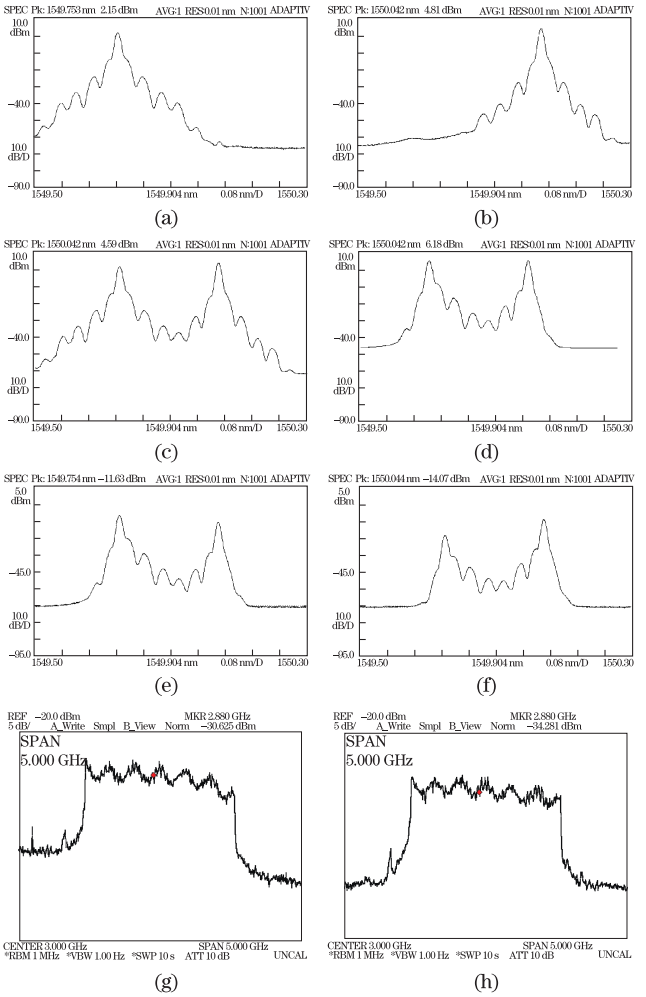

Fig. 3. (a) Optical SCFDM signal at Pol-X; (b) optical SCFDM signal at Pol-Y; (c) DSB-PI-SCFDM signal after multiplexing by PBC; (d) SSB-PI-SCFDM signal after OBPF; (e) Pol-X' optical signal; (f) Pol-Y' optical signal; (g) electrical SCFDM signal at Pol-X'; (h) electrical SCFDM signal at Pol-Y'.

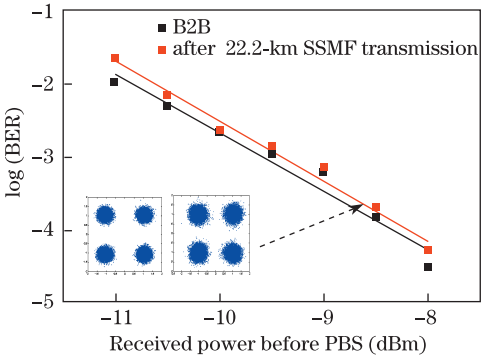

Fig. 4. BER performance of the SSB-PI-SCFDM signal under B2B and 22.2-km SSMF transmission.

Each BER is calculated on the basis of 2000 SCFDM symbols, which include more than 1.7×10^6 bits for both polarizations. The received optical power before multiplexing using the PBS is about –10 dBm, which enables deriving a BER of 1×10^{-3}. The comparison of the B2B and 22.2-km SSMF transmission curves indicates that

the chromatic dispersion-induced penalty is negligible.

In conclusion, we propose a novel PI approach for SCFDM-PON and OFDM-PON using direct detection. This approach significantly reduces bandwidth requirements for electrical and optical components while realizing a high-flexibility and low-complexity MIMO algorithm. Downstream SSB PI-SCFDM-PON transmission is experimentally demonstrated.

This work was supported by the National "973" Program of China (Nos. 2010CB328201 and 2010CB328202), the National Natural Science Foundation of China (Nos. 60907030, 60736003, and 60931160439), and the National "863" Program of China (No. 2011AA01A106).

References

1. C. Zhang, J. Li, F. Zhang, Y. He, H. Wu, and Z. Chen, Opt. Express **18,** 24556 (2010).
2. C. W. Chow, C. H. Yeh, C. H. Wang, C. L. Wu, S. Chi, and C. Lin, IEEE J. Sel. Areas Commun. **28,** 800 (2010).
3. J. L. Wei, A. Hamié, R. P. Gidding, E. Hugues-Salas, X. Zheng, S. Mansoor, and J. M. Tang, Opt. Express **18,** 8556 (2010).
4. D. Qian, N. Cvijetic, J. Hu, and T. Wang, Photon. Technol. Lett. **21,** 1265 (2009).
5. T. Duong, N. Genay, M. Ouzzif, J. Le Masson, B. Charbonnier, P. Chanclou, and J. C. Simon, Photon. Technol. Lett. **12,** 790 (2009).
6. D. Qian, J. Hu, P. Ji, T. Wang, and M. Cvijetic, in *Proceedings of OFC/NFOEC 2008* OWH4 (2008).
7. P. Tien, Y. Lin, and M. C. Yuang, in *Proceedings of OFC 2009* OMV2 (2009).
8. C. Chow, C. Yeh, C. Wang, F. Shih, C. Pan, and S. Chi, Opt. Express **16,** 12096 (2008).
9. Y. M. Lin, in *Proceedings of OFC 2007* OThD7 (2007).
10. H. Chien, R. Chen, M. Huang, and G. Chang, in *Proceedings of OFC/NFOEC 2011* OTuK2 (2011).
11. D. Qian, N. Cvijetic, J. Hu, and T. Wang, J. Lightwave Technol. **28,** 484 (2010).
12. D. Qian, N. Cvijetic, J. Hu, and T. Wang, in *Proceedings of OFC 2009* OMV3 (2009).
13. N. Cvijetic, N. Prasad, D. Qian, J. Howard, and T. Wang, in *Proceedings of OFC/NFOEC 2011* OTuK6 (2011).
14. S. L. Jansen, I. Morita, T. C. Schenk, and H. Tanaka, J. Opt. Netw. **7,** 173 (2008).
15. J. Li, C. Zhao, S. Zhang, F. Zhang, and Z. Chen, Photon. Technol. Lett. **22,** 1814 (2010).
16. Y. Han and G. Li, Opt. Express **13,** 7527 (2005).